Schejter, A., & Margalit, R. (1970) *FEBS Lett. 10*, 179.
Shaw, R. G., & Hartzell, C. R. (1976) *Biochemistry 15*, 1909.
Smith, L., & Conrad, H. (1956) *Arch. Biochem. Biophys. 63*, 403.
Smith, H. T., Staudenmayer, N., & Millett, F. (1977) *Biochemistry 16*, 4971.
Steinhardt, J., & Reynolds, J. A. (1969) *Multiple Equilibria in Proteins*, Academic Press, New York.
Stellwagen, E. (1968) *Biochemistry 7*, 2496.
Stellwagen, E., & Shulman, R. G. (1973) *J. Mol. Biol. 75*, 683.
Stellwagen, E., & Cass, R. D. (1975) *J. Biol. Chem. 250*, 2095.
Stellwagen, E., Smith, L. M., Cass, R., Ledger, R., & Wilgus, H. (1977) *Biochemistry 16*, 3672.
Swanson, R., Trus, B. L., Mandel, N., Mandel, G., Kallai, O. B., & Dickerson, R. E. (1977) *J. Biol. Chem. 252*, 759.
Takano, T., Trus, B. L., Mandel, N., Mandel, G., Kallai, O. B., Swanson, R., & Dickerson, R. E. (1977) *J. Biol. Chem. 252*, 776.
Tsou, C. L. (1951) *Biochem. J. 49*, 362.
Wütrich, K. (1971) in *Probes of Structure and Function of Macromolecules and Membranes* (Chance, B., Yonetani, T., & Mildvan, A. S., Eds.) Vol. 2, p 465, Academic Press, New York.

Resonance Raman Spectra and Optical Properties of Oxidized Cytochrome Oxidase†

Gerald T. Babcock*,‡ and Irving Salmeen*

ABSTRACT: Raman spectra of oxidized cytochrome oxidase and its inhibitor complexes with cyanide and formate have been recorded by using 441.6-nm HeCd laser excitation. Photoreduction effects were avoided by flowing the protein samples through the scattering volume. As an aid in the interpretation of the protein data, Raman spectra of low- and high-spin ferric heme *a* complexes dissolved in water or in non-hydrogen-bonding organic solvents were recorded. The model compound data demonstrate that heme *a* vibrational bands in the 1540–1660-cm^{-1} region are sensitive to iron spin state and indicate that the Raman spectrum of oxidized cytochrome oxidase obtained with 441.6-nm excitation is due primarily to vibrations of low-spin cytochrome a^{3+}. The spectra of the inhibitor complexes of the enzyme are consistent with this interpretation. The selective enhancement of cytochrome a^{3+} vibrational modes under these conditions is rationalized by using simple considerations of the Raman excitation profile and the optical spectra of cytochromes *a* and a_3 deduced by W. H. Vanneste [(1966) *Biochemistry 5*, 838–848]. In contrast to the Raman spectrum of reduced cytochrome a_3, those of oxidized and reduced cytochrome *a* do not show a well-defined heme *a* formyl vibration in the 1670-cm^{-1} region. The model compound data indicate that either hydrogen bonding or lack of conjugation of the formyl π electrons with the porphyrin π system can account for this observation. The implications which this may have for heme–heme interaction in the protein are discussed.

Cytochrome oxidase, the terminal oxidase in mitochondrial respiration, contains two heme *a* bound iron atoms and two copper atoms. In the protein, the hemes *a*, as well as the copper atoms, are functionally and magnetically distinct as reflected in the cytochrome aa_3 nomenclature (Palmer et al., 1976; Erecinska & Wilson, 1978). Cytochrome *a* comprises one of the hemes *a* and its protein surroundings and is a site of cytochrome *c* oxidation. Its iron is low spin in both the resting and fully reduced enzyme with histidine residues as the probable occupants of the fifth and sixth coordination positions (Babcock et al., 1979). Oxygen reduction occurs at cytochrome a_3; the heme *a* iron involved in this reaction is high spin and, in its ferric state, strongly antiferromagnetically coupled to one of the copper atoms (Falk et al., 1977; Tweedle et al., 1978). The second copper is magnetically isolated and, in its cupric state, shows an EPR[1] spectrum with an unusually small hyperfine splitting. The function and ligands of this copper are uncertain, although it may play a part, along with cytochrome *a*, in cytochrome *c* oxidation (Powers et al., 1979; Chan et al., 1979).

Electron paramagnetic resonance, magnetic circular dichroism, and magnetic susceptibility measurements have provided much of the information on cytochrome oxidase at the molecular level. These methods supply detailed information on the paramagnetic ferric, ferrous, and cupric species in the enzyme but are not very sensitive to the geometry and bonding of the unusual peripheral substituents of the heme *a* porphyrin ring (Babcock et al., 1979). The importance of these substituents, a formyl at ring position 8 and a hydroxyfarnesylethyl group at position 2, has been suggested by the reconstitution experiments of Hill & Wharton (1978). For *Pseudomonas aeruginosa* cytochrome oxidase, they observed that reconstitution with either heme *a* or heme d_1 in the enzyme active site restored function; reconstitution with protoheme did not produce oxidase activity.

Resonance Raman spectroscopy yields porphyrin structural information (Spiro, 1974; Warshel, 1977) which is complementary to that obtained by the magnetic techniques described above. For example, the vibrations of porphyrin ring substituents can be observed directly (Salmeen et al., 1973; Lutz, 1977), insight into the planarity of the porphyrin ring can be obtained (Spaulding et al., 1975; Spiro, 1974), and porphyrin

† From the Department of Chemistry, Michigan State University, East Lansing, Michigan 48824 (G.T.B.), and the Research Staff, Ford Motor Company, Dearborn, Michigan 48121 (I.S.). *Received January 17, 1979.*
‡ Supported by a Cottrell Research Grant from the Research Corporation and a Michigan State University Biomedical Research Support Grant.

[1] Abbreviations used: EPR, electron paramagnetic resonance; Hepes, *N*-2-hydroxyethylpiperazine-*N'*-2-ethanesulfonic acid; MCD, magnetic circular dichroism; Me_2SO, dimethyl sulfoxide.

0006-2960/79/0418-2493$01.00/0

metal–axial ligand properties can be determined independent of the magnetic state of the metal (Yamamoto et al., 1973; Ozaki et al., 1976; Burke et al., 1978). We have shown previously that this technique is particularly useful in the study of cytochrome oxidase when the excitation frequency is within the Soret band (Salmeen et al., 1978). With 441.6-nm excitation, the Raman spectrum of the reduced enzyme shows a band near 1672 cm^{-1} due to the heme *a* formyl vibration which is not resonance enhanced with excitation within the α or β bands (Kitagawa et al., 1977; Chan et al., 1979). We assigned the formyl vibration observed for the reduced oxidase to high-spin cytochrome a_3^{2+} and showed that ligand binding at this site results in the disappearance of the 1672-cm^{-1} band, possibly as a result of a shift in the conformation of the formyl group. The potential importance of this geometry shift to the oxygen binding and reduction reactions catalyzed by the cytochrome a_3 site has been discussed recently (Babcock & Chang, 1979).

The oxidase Raman results we have reported to date pertain only to the reduced enzyme and its partially reduced inhibitor complexes (Salmeen et al., 1978). The oxidized enzyme and its inhibitor complexes are more difficult to study by Raman spectroscopy because of photoreduction of one or both of the hemes *a* in the laser beam (Adar & Yonetani, 1978; Salmeen et al., 1978). In the experiments reported here, we have used a flowing sample to minimize the concentration of photoreduced enzyme in the scattering volume and have obtained spectra of the oxidized species. As an aid in the interpretation of these results, we have used Raman spectra of low- and high-spin ferric heme *a* complexes dissolved in water or in organic solvent. The data indicate that several heme *a* vibrational bands are sensitive to iron spin state, that the Raman spectrum of oxidized cytochrome oxidase obtained under 441.6-nm excitation is primarily that of cytochrome *a*, and that its heme *a* formyl group vibration is at most only weakly resonance enhanced. The conclusion that the oxidase Raman spectra obtained with 441.6-nm excitation are dominated by cytochrome *a* vibrations is consistent with simple considerations of the Raman excitation profile in conjunction with optical spectra of cytochromes *a* and a_3 deduced by Vanneste (1966).

Materials and Methods

Cytochrome oxidase and heme *a* were isolated and inhibitor complexes of the oxidized enzyme were prepared as described previously (Babcock et al., 1976). Fairly dilute protein samples, typically 40 μM in heme *a*, were used so that optical spectra could be recorded in the Raman sample cuvette. Chemicals were obtained from standard commercial sources. Imidazole was recrystallized from benzene or from ethanol. The nonionic detergent, Brij 35 (Sigma, St. Louis, MO), was used as the solubilizing detergent for cytochrome oxidase because of its lack of fluorescent impurities. The optical properties of both oxidized (λ_{max} (vis) 599 nm; λ_{max} (Soret) 421 nm) and reduced (λ_{max} (vis) 604 nm; λ_{max} (Soret) 443 nm) cytochrome oxidase were not altered by the use of this detergent. Furthermore, Brij 35 was nearly as effective as Tween 80 in restoring cytochrome *c* oxidase activity to lipid depleted preparations of the protein. However, Brij 35 is susceptible to slow air oxidation and consequently solutions of the detergent were prepared and stored under argon.

Raman spectra were recorded by using the 441.6-nm line of an RCA LD2186 HeCd laser and the spectrometer described previously (Salmeen et al., 1978). Reported frequencies are accurate to ±2 cm^{-1}; the scan rate used in recording spectra was 1 cm^{-1}/s. Spectra of oxidized cytochrome oxidase and its inhibitor complexes were recorded by flowing

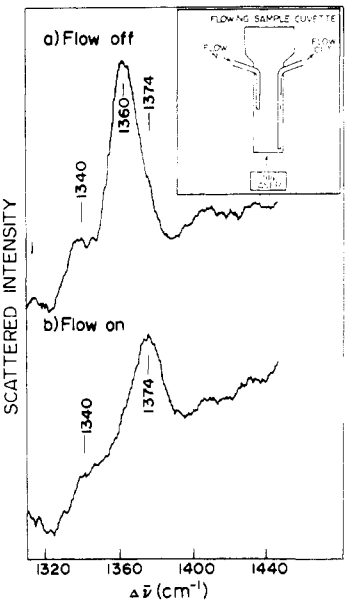

FIGURE 1: Raman spectra of (a) stationary and (b) flowing samples of resting cytochrome oxidase dissolved in 0.5% Brij 35, 0.05 M Hepes, pH 7.4. Inset: schematic diagram of the flowing sample cuvette showing the relationship between flow and the illumination optics; scattered light is collected normal to the plane of the figure.

the protein solution through the scattering volume by using a 5 × 10 mm cuvette modified as shown in the inset of Figure 1. The sample is pumped from the bottom and returned to the cuvette from the top by using a Gilson Minipuls peristaltic pump. Flow rates were about 25 mL/min; the total sample volume was 4.5 mL. The sample temperature was maintained near 10 °C in all experiments. The effectiveness of this arrangement in eliminating photoreduction artifacts is illustrated in Figure 1 which shows the Raman oxidation state marker region (Yamamoto et al., 1973; Spiro, 1974) for flowing and nonflowing samples of oxidized cytochrome oxidase. For the stationary sample, extensive photoreduction is evident as a 1361-cm^{-1} peak and weak 1374-cm^{-1} shoulder; for the flowing sample, the 1361-cm^{-1} band is eliminated. The flow cell was checked for flow artifacts by recording spectra for static and flowing samples of oxidized cytochrome *c*. Identical results were obtained under the two sets of experimental conditions.

EPR spectra were recorded at X band with a Varian E4 EPR spectrometer fitted with an Oxford Instruments ESR-9 liquid helium cryostat. Optical spectra were recorded by using either Cary 17 or McPherson EU-707D recording spectrophotometers.

Results

Resonance Raman spectra (λ_{ex} 441.6 nm), recorded for flowing samples of oxidized cytochrome oxidase and its inhibitor complexes with cyanide and formate, are shown in Figure 2. For comparison, a spectrum of the dithionite reduced enzyme is also shown. The absorption spectra recorded for these species are shown in Figure 3 and the 441.6-nm exciting frequency is indicated.

Relative to the Raman spectrum of the reduced enzyme, the signal-to-noise ratios of those obtained for the oxidized species are poorer. With 441.6-nm excitation, the resonance Raman scattered intensity is expected to be dominated by resonance with the Soret band excited state and should be approximately proportional to *R*, defined as

$$R = \epsilon^2/[(\nu - \nu_0)^2 + \Gamma^2] \quad (1)$$

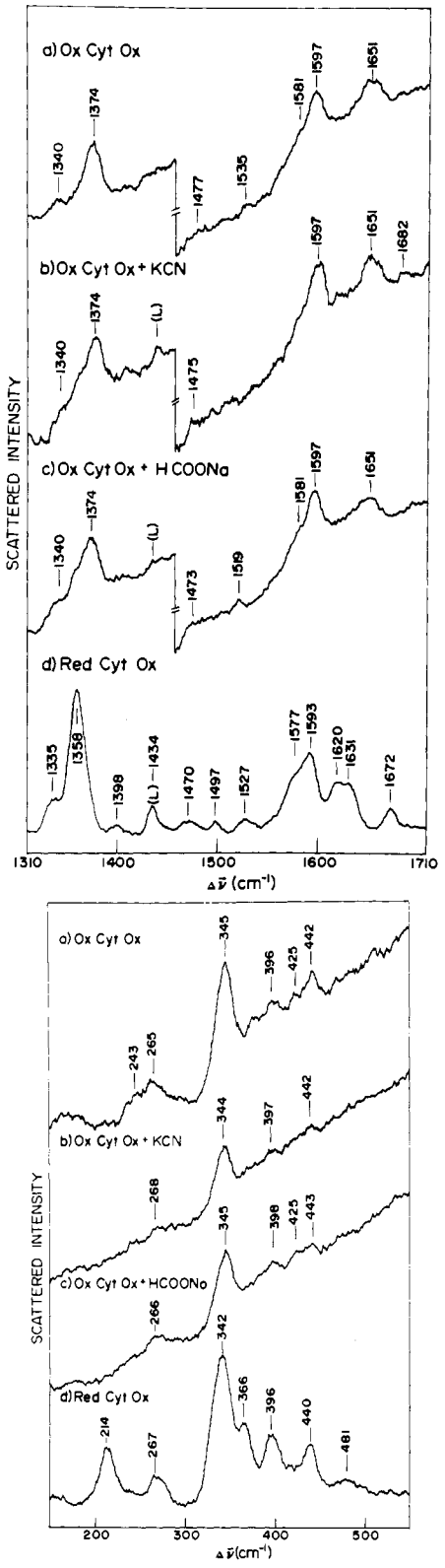

FIGURE 2: Raman spectra of (a) oxidized cytochrome oxidase, its inhibitor complexes with (b) cyanide and (c) formate, and (d) reduced cytochrome oxidase in the low (bottom panel) and high (top panel) frequency regions. In a, b, and c, the heme *a* concentration was 45 μM; in d the sample was 25 μM in heme *a*. The cyanide concentration was 5 mM and the formate concentration was 60 mM. Stock solutions of each inhibitor were neutralized prior to addition to the protein solution. In d, the line at 1434 cm^{-1} corresponds to laser fluorescence. The overall instrument sensitivity was the same for all four samples.

where ϵ is the molar extinction coefficient at the frequency, ν, of the Soret band absorption maximum, ν_0 is the exciting laser frequency, and Γ is the Soret band width at half-

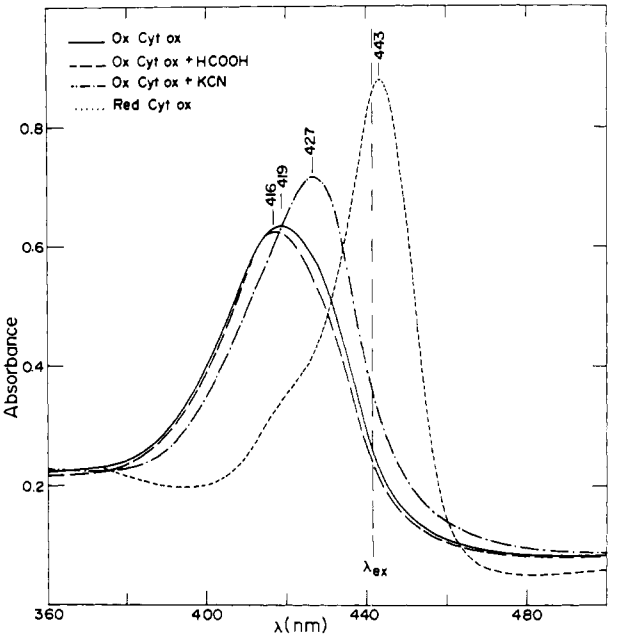

FIGURE 3: Soret optical absorption spectra of oxidized cytochrome oxidase, of its inhibitor complexes with formate and cyanide, and of reduced cytochrome oxidase. The protein concentration was approximately 4 μM (in cytochrome oxidase) for each of the spectra.

maximum (Albrecht & Hutley, 1971; Shelnutt et al., 1977). Using the Soret extinction coefficients of oxidized and reduced cytochrome oxidase (Lemberg, 1969) and determining band widths from Figure 3, we estimate that the vibrations of the reduced protein are resonance enhanced five to six times more strongly than those of the oxidized enzyme when ν_0 = 22 649 cm^{-1} (441.6 nm). The main noise source is due to the fluorescence background which has about four times the intensity in the flowing oxidized samples compared with the stationary reduced species. Consequently, the noise amplitude, proportional to the square root of the average fluorescence intensity, about doubles.

The spectrum of the oxidized enzyme (Figure 2a) shows the oxidation state marker band at 1374 cm^{-1} with no shoulder apparent at 1360 cm^{-1}. The peak at 1597 cm^{-1} is broadened slightly on the low frequency side, indicating weak unresolved bands in the 1580-cm^{-1} region. For the 1651-cm^{-1} peak, a similar broadening to low frequency is observed. A spectrum of a second sample of the oxidized oxidase, from a different preparation of the enzyme, is shown in Figure 4a and demonstrates typical levels of reproducibility for the principle features of the spectrum. Raman spectra of the oxidized enzyme dissolved in sodium cholate, an ionic detergent, were identical with those recorded for the Brij 35 solubilized enzyme. Addition of cyanide, which generates the low-spin cytochrome a_3^{3+}·CN^- species, produces a spectrum which is similar to that of the oxidized enzyme except that there is less intensity on the low frequency side of the peaks at 1597 and 1651 cm^{-1} and, consequently, these bands are sharpened. Formate addition, producing the high-spin cytochrome a_3^{3+}·HCOOH species, results in a spectrum which resembles that of the oxidized enzyme in that the 1597- and 1651-cm^{-1} bands are broadened on the low frequency side. Using the ratio of scattered intensity (I) at 1581 cm^{-1} to that at 1597 cm^{-1} as a measure of these band shape changes, we estimate that $I(1581\ cm^{-1})/I(1597\ cm^{-1})$ = 0.7 for the oxidized enzyme and its formate complex; for the cyanide bound enzyme, this ratio decreases to 0.5. The spectra of both inhibitor complexes show weak shoulders on the low frequency side of the 1374-cm^{-1}

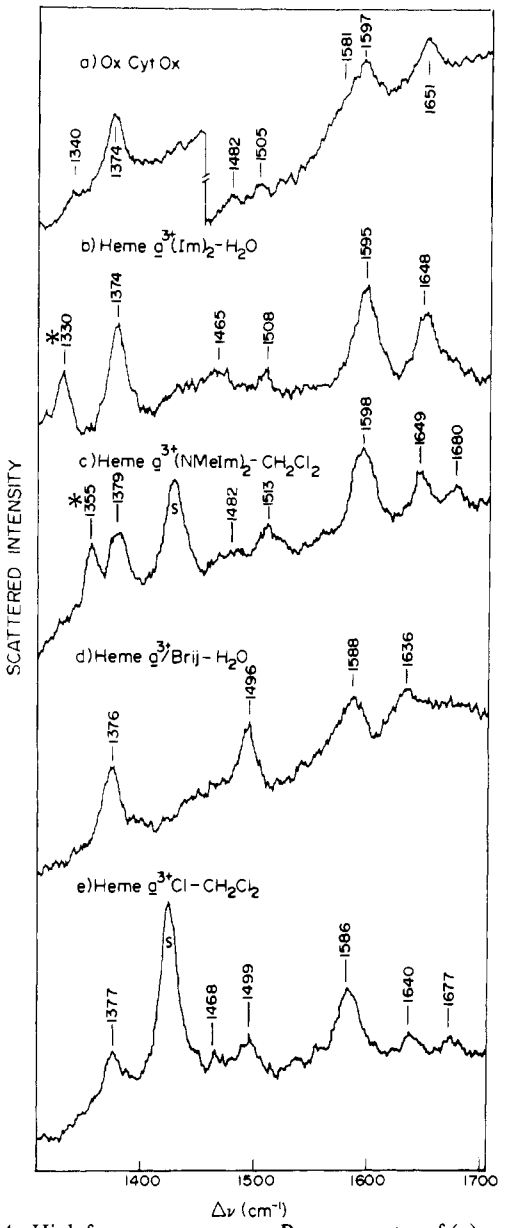

FIGURE 4: High frequency resonance Raman spectra of (a) oxidized cytochrome oxidase, (b) ferric heme *a* bis(imidazole) dissolved in water, (c) ferric heme *a* bis(*N*-methylimidazole) dissolved in methylene chloride, (d) ferric heme *a* dissolved in 2% Brij 35 detergent, and (e) ferric heme *a* chloride dissolved in methylene chloride. Soret band absorption maxima for the low-spin species occurred at 420–422 nm; for the high-spin species at 408–410 nm. In c and e, methylene chloride bands are indicated by an "S"; in b and c, bands which appear in the nonresonance enhanced Raman spectra of concentrated solutions of imidazole and *N*-methylimidazole are indicated by an asterisk. The heme *a* concentration for the low-spin species (spectra *b* and *c*) was approximately 50 μM and the axial ligand concentration was 0.3 M. In b, 5 mM sodium dodecyl sulfate was also present to prevent heme *a* aggregation. For the high-spin species (spectra d and e), the heme *a* concentration was approximately 80 μM. The instrument sensitivity was three times higher for the model compounds (b–e) than that for the oxidized cytochrome oxidase spectrum (a).

oxidation state marker band which could reflect approximately 5% photoreduction in these samples. Because the 1358-cm^{-1} band is the most intense band in the spectrum of the reduced enzyme (Figure 2d), a minor contamination (<10%) has a negligible effect on the bands in the 1500–1700-cm^{-1} region in the spectra of the oxidized inhibitor complexes.

The formyl band, which occurs at 1672 cm^{-1} in the spectrum of the reduced protein, is apparently absent from the spectra of the oxidized enzyme and of its formate–inhibitor complex. For the cyanide derivative, there is a suggestion of a weak band (less than one-tenth the intensity of the 1597-cm^{-1} band) in the 1680-cm^{-1} region. In the low frequency region, the Raman spectra of the three oxidized species are similar; the 214- and 366-cm^{-1} vibrations observed for the reduced protein and attributed to cytochrome a_3^{2+} (Salmeen et al., 1978) are not apparent in the spectra of the oxidized species.

The results shown in Figure 2 indicate that the Raman spectra of oxidized cytochrome oxidase and its inhibitor complexes obtained with 441.6-nm excitation are relatively insensitive to the spin state of cytochrome a_3^{3+}. The position of the major bands and their relative intensities are unaffected; only the broadening to low frequency of the 1597- and 1651-cm^{-1} bands appears to correlate with cytochrome a_3^{3+} spin state. The minor influence of a_3^{3+} spin state on the oxidized oxidase Raman spectrum is in contrast to the effects of spin state on the Raman spectra of heme *a* complexes obtained with 514.5-nm excitation (Kitagawa et al., 1977) and of other heme proteins recorded with excitation near the Soret (Yamamoto et al., 1973; Verma & Bernstein, 1974; Champion et al., 1978) or near the α–β bands (Spiro, 1974; Spaulding et al., 1975).[2] To establish the sensitivity to spin state of heme *a* resonance Raman spectra obtained with 441.6-nm excitation, we recorded resonance Raman spectra of low- and high-spin ferric heme *a* derivatives. Heme *a* bis(imidazole) and heme *a* bis(*N*-methylimidazole) are low spin and heme *a* in aqueous Brij 35 and heme *a* chloride in CH_2Cl_2 are high spin as judged by MCD and EPR spectroscopies (Babcock et al., 1979; Babcock & Chang, 1979). The Raman spectra recorded for these compounds are shown in Figure 4. The low-spin species (spectra 4b and 4c) show strong bands at 1595–1598 and 1648–1649 cm^{-1}. The corresponding bands in the spectra of the high-spin species (4d and 4e) are shifted 10–12 cm^{-1} to lower frequencies and indicate that the Raman sensitivity to spin state observed for other hemes and heme proteins obtains for heme *a* as well.

Following a recent suggestion (Zobrist & La Mar, 1978) that ferric porphyrins dissolved in dimethyl sulfoxide are six coordinate and high spin and, consequently, more appropriate models for high-spin ferric heme proteins, we also recorded the Raman spectrum of heme *a* dissolved in this solvent. In the high-frequency region, bands were observed at 1373, 1498, 1583, 1635, and 1671 cm^{-1}. Upon conversion to the low-spin heme *a* bis(*N*-methylimidazole) complex, bands in the 1550–1660-cm^{-1} region occurred at 1594 and 1651 cm^{-1}. The intensity pattern of the high frequency bands for the high- and low-spin heme *a* species in Me_2SO were somewhat different from those observed with the solvents used in Figure 4. Nonetheless, these results are in qualitative agreement with the water and methylene chloride data in that a spin-state dependency in the Raman parameters is evident.

A further interesting aspect of the spectra of Figure 4 is the appearance of a well-resolved vibrational band in the 1680-cm^{-1} region for both high- and low-spin ferric heme *a* complexes in the non-hydrogen-bonding solvent, methylene chloride. In contrast, the heme *a* complexes in aqueous solution show only broadening on the high frequency side of the peak at 1649 cm^{-1} in the spectrum of low-spin heme *a* species (Figure 4b) and of the peak at 1636 cm^{-1} in the spectrum of the high-spin species (Figure 4d). We attribute the broadening in the aqueous samples and the well-resolved high frequency band in the nonaqueous samples to the heme *a* formyl group.

[2] This empirical correlation may not reflect spin state per se, but rather the geometry and bonding imposed by the various spin states (Spaulding et al., 1975; Spiro & Burke, 1976).

Table I: Spectral and Raman Parameters–Cytochrome a and a_3 Species[a]

species	spin	[λ_{max} (nm)] ν (cm^{-1})	Γ (cm^{-1})	ϵ (mM^{-1} cm^{-1})	$R \times 10^3$ (ν_0 = 22 649 cm^{-1})
a_3^{3+}	5/2	[414] 24154	800	81	2.2
$a_3^{3+}\cdot CN^-$	1/2	[427] 23419	550	65	4.7
$a_3^{3+}\cdot HCOOH$	5/2	[414] 24154	750	98	3.3
a^{3+}	1/2	[427] 23419	800	120	12.3
a_3^{2+}	2	[442.5] 22598	400	125	96.0
$a_3^{2+}\cdot CN^-$	0	[441] 22675	400	96	57.1
a^{2+}	0	[444] 22522	550	113	40.3

[a] Spin states from Babcock et al. (1976); spectral parameters from Vanneste (1966).

The solvent dependent differences between the two types of spectra most likely reflect the formation of hydrogen bonds to the formyl carbonyl group in the aqueous systems (Lutz, 1977). Except for the large effects on the carbonyl band, the solvent has only a minor influence on the frequencies of the other bands.

Discussion

The model compound data provide a guide in the interpretation of the Raman data for oxidized cytochrome oxidase and its inhibitor complexes shown in Figure 2. In the oxidized enzyme–cyanide complex, both cytochromes a and a_3 are low spin (Tweedle et al., 1978) and the observed Raman spectrum, with bands at 1597 and 1651 cm^{-1}, can be confidently assigned to the low-spin heme a species. These two bands are similar to those observed in the spectra of the low-spin heme a complexes shown in Figure 4. Both the fully oxidized enzyme and the oxidized enzyme–formate complex contain one low-spin and one high-spin heme a (Nicholls, 1975; Palmer et al., 1976, 1978). We attribute the strong bands at 1597 and 1651 cm^{-1} to low-spin cytochrome a^{3+} and the weak contribution on the low frequency side of each of these bands to weakly resonance enhanced vibrations of high-spin cytochrome a_3^{3+}, with bands analogous to those shown by the high-spin heme a complexes in Figure 4. This interpretation indicates that, with 441.6-nm excitation, cytochrome a^{3+} vibrations are more strongly resonance enhanced than those of cytochrome a_3^{3+}.

The selective enhancement of cytochrome a^{3+} vibrations can be understood within the context of the optical properties of cytochromes a and a_3 determined by Vanneste (1966). As discussed above (see Results), the resonance Raman scattered intensity is approximately proportional to the quantity R, defined in eq 1, when the exciting frequency is near the Soret band. Using values for ϵ, ν, and Γ for cytochromes a and a_3 obtained from Vanneste (1966), we calculated the expected enhancements for the vibrations of the individual a and a_3 species. These are compiled in Table I. For the oxidized enzyme, the vibrations of low-spin cytochrome a are estimated to be more strongly enhanced, by a factor of five, compared with those of high-spin cytochrome a_3^{3+}. Approximately the same enhancement ratio applies to the formate complexed enzyme. In the cyanide-inhibited enzyme, where both hemes a are low spin and absorb maximally at 427 nm, the contribution of cytochrome $a_3^{3+}\cdot CN^-$ to the observed Raman spectrum is expected to be roughly 40–50% of that of cytochrome a^{3+}. This is likely to be a low estimate for the $a_3^{3+}\cdot CN^-$ contribution since the extinction coefficient given by Vanneste, 65 mM^{-1} cm^{-1}, is somewhat lower than we would expect for low-spin heme a. Some caution, therefore, should be exercised in using Vanneste's data and eq 1 for detailed quantitative estimates of enhancement ratios. Several approximations are involved in the calculation of R, including neglect of vibronic coupling between Soret band transitions and other electronic transitions in the molecule. With Soret excitation, this is a reasonable assumption (Shelnutt et al., 1977), but, nonetheless, its use should be stated explicitly. Vanneste based his analysis on a photochemical action spectrum which introduces uncertainties in the estimates of ϵ and Γ. Nevertheless, the frequencies of the absorption maxima are probably correct as indicated by MCD data (Babcock et al., 1976), and our Raman results indicate that the other parameters are reasonable.

Vanneste's (1966) treatment, as well as similar analyses performed by Yonetani (1960) and Horie & Morrison (1963), is based on a model of the oxidase in which each of the two hemes a of the protein absorbs independently and is not influenced by redox or ligand changes at the second heme. The recent observation of heme–heme interaction in the enzyme has made a reassessment of the validity of this analysis necessary (Malmstrom, 1973; Erecinska & Wilson, 1978; Lanne & Vanngard, 1978). The possible occurrence of exciton interaction between the two hemes a has also been postulated (Adar & Erecinska, 1978; Adar & Yonetani, 1978) and, if in effect, would produce interaction effects in the oxidase optical properties. The analysis of the Raman data reported here, as well as an analogous treatment of MCD data for the oxidase (Babcock et al., 1976), indicates, however, that the spectrally noninteracting model developed by Yonetani, Horie & Morrison, and Vanneste provides a satisfactory explanation of the experimental observations. Thus the principal mode by which heme–heme interaction is expressed in the protein does not appear to involve a strong coupling between the optical parameters of the two hemes.

An alternative explanation for heme–heme interaction in cytochrome oxidase invokes redox coupling between cytochromes a and a_3 such that the electron affinity of each of the metal centers in the enzyme depends on the chemical status of the other species present (Nicholls & Chance, 1974; Wikstrom et al., 1976). Recent reductive titration data obtained for cytochrome oxidase and its carbon monoxide complex provide experimental support for this hypothesis (Babcock et al., 1978). The molecular mechanism responsible for this phenomenon is unknown. Porphyrin-bound metal redox potentials are quite sensitive to the resonance and inductive properties of the ring substituents (Caughey et al., 1966; Moore & Williams, 1977), however, which suggests that redox potential interaction in the oxidase may involve redox state or protein control of the conformation of the heme a formyl group and, hence, its electron-withdrawing properties (Babcock et al., 1979). A formyl conformation such that it lies in the plane of the porphyrin ring and is conjugated with the porphyrin π system would maximize its electron-withdrawing effects and, consequently, increase the heme a iron redox potential; rotation of the formyl out of plane would lessen this resonance effect and decrease the iron electron affinity (Seybert et al., 1977). Crystallographic data on several porphyrin systems provide support for this idea: both vinyl and carbonyl porphyrin ring substituents possess at least a limited degree of rotational freedom and can shift geometry to accommodate constraints imposed by their immediate environment (Little et al., 1975; Hamor et al., 1965). In previous Raman work on reduced cytochrome oxidase (Salmeen et al., 1978), we found that the heme a formyl vibration was observed as a well-resolved, resonance enhanced band near 1670 cm^{-1} for high-spin cytochrome a_3, but could not be

observed in the spectrum of low-spin cytochrome *a*. Moreover, when cyanide was bound to cytochrome a_3^{2+} to produce the low-spin ferrous species, the 1670-cm^{-1} band disappeared. This observation was interpreted as indicative of movement of the formyl group out of the porphyrin plane during ligand binding. Subsequent model studies supported this hypothesis and suggested that the conformation of the formyl is linked to the ferrous iron spin state (Babcock et al., 1979).

The electron-withdrawing effect of the formyl group is subject to a second type of control mechanism, one which would be exerted by hydrogen-bond formation to the carbonyl oxygen. The spectra for both high- and low-spin ferric heme *a* model compounds (Figure 4) show a well-resolved formyl band near 1680 cm^{-1} in the non-hydrogen-bonding solvent, methylene chloride, but a poorly resolved band near 1660 cm^{-1} in water. The broadening and lower frequency of the formyl band in water are most likely the result of hydrogen bonding to the formyl carbonyl oxygen (Lutz, 1977). In the spectra of oxidized cytochrome oxidase (Figures 2a and 4a), the absence of a well-resolved formyl vibration could be due to either hydrogen-bond formation to the carbonyl of cytochrome *a*, causing the formyl band to be obscured by the 1651-cm^{-1} band, or to poor coupling between the formyl and porphyrin π electrons imposed by a nonplanar geometry. At present we are unable to decide between these two effects or whether, in fact, both are operative. It appears, however, that the formyl of cytochrome a_3 and that of cytochrome *a* are subject to different environmental constraints. This, as well as other effects, such as one analogous to the apparent protein control of the iron–porphyrin plane distance in aquomethemoglobin α and β chains (Ladner et al., 1977) may play a role in mediating heme–heme interaction in cytochrome oxidase.

References

Adar, F., & Erecinska, M. (1978) *Biochemistry 17*, 5484–5488.

Adar, F., & Yonetani, T. (1978) *Biochim. Biophys. Acta 502*, 80–86.

Adar, F., Gouterman, M., & Aronowitz, S. (1976) *J. Phys. Chem. 80*, 2184–2191.

Albrecht, A. C., & Hutley, M. C. (1971) *J. Chem. Phys. 55*, 4438–4443.

Babcock, G. T., & Chang, C. K. (1979) *FEBS Lett. 97*, 358–362.

Babcock, G. T., Vickery, L. E., & Palmer, G. (1976) *J. Biol. Chem. 251*, 7907–7919.

Babcock, G. T., Vickery, L. E., & Palmer, G. (1978) *J. Biol. Chem. 253*, 2400–2411.

Babcock, G. T., Van Steelandt, J., Palmer, G., Vickery, L. E., & Salmeen, I. (1979) *Developments in Biochemistry, 5: Cytochrome Oxidase* (King, T. E., Orii, Y., Chance, B., & Okunuki, K., Eds.) Elsevier, Amsterdam, pp 105–115.

Burke, J. M., Kincaid, J. R., & Spiro, T. G. (1978) *J. Am. Chem. Soc. 100*, 6077–6083.

Caughey, W. S., Fujimoto, W. Y., & Johnson, B. P. (1966) *Biochemistry 5*, 3830–3843.

Champion, P. M., Gunsalus, I. C., & Wagner, G. C. (1978) *J. Am. Chem. Soc. 100*, 3743–3751.

Chan, S. I., Bocian, D. F., Brudvig, G. W., Morse, R. H., & Stevens, T. H. (1979) *Developments in Biochemistry, 5: Cytochrome Oxidase* (King, T. E., Orii, Y., Chance, B., & Okunuki, K., Eds.) Elsevier, Amsterdam, pp 177–188.

Erecinska, M., & Wilson, D. F. (1978) *Arch. Biochem. Biophys. 188*, 1–14.

Falk, K. E., Vanngard, T., & Angstrom, J. (1977) *FEBS Lett. 75*, 23–27.

Hamor, T. A., Caughey, W. S., & Hoard, J. L. (1965) *J. Am. Chem. Soc. 87*, 2305–2312.

Hill, K. E., & Wharton, D. C. (1978) *J. Biol. Chem. 253*, 489–495.

Horie, S., & Morrison, M. (1963) *J. Biol. Chem. 238*, 2859–2865.

Kitagawa, T., Kyogoku, K., & Orii, Y. (1977) *Arch. Biochem. Biophys. 181*, 228–235.

Ladner, R. C., Heidner, E. J., & Perutz, M. F. (1977) *J. Mol. Biol. 114*, 385–414.

Lanne, B., & Vanngard, T. (1978) *Biochim. Biophys. Acta 501*, 449–457.

Lemberg, M. R. (1969) *Physiol. Rev. 49*, 48–121.

Little, R. G., Dymock, K. R., & Ibers, J. A. (1975) *J. Am. Chem. Soc. 97*, 4532–4539.

Lutz, M. (1977) *Biochim. Biophys. Acta 460*, 408–430.

Malmstrom, B. G. (1973) *Q. Rev. Biophys. 6*, 389–431.

Moore, G. R., & Williams, R. J. P. (1977) *FEBS Lett. 79*, 229–232.

Nicholls, P. (1975) *Biochim. Biophys. Acta 396*, 24–35.

Nicholls, P., & Chance, B. (1974) in *Molecular Mechanisms of Oxygen Activation* (Hayaishi, O., Ed.) pp 479–534, Academic Press, New York.

Ozaki, Y., Kitagawa, T., Kyogoku, Y., Shimada, T., Iizuka, T., & Ishimura, Y. (1976) *J. Biochem. (Tokyo) 80*, 1447–1451.

Palmer, G., Babcock, G. T., & Vickery, L. E. (1976) *Proc. Natl. Acad. Sci. U.S.A. 73*, 2206–2210.

Palmer, G., Antalis, T., Babcock, G. T., Garcia-Iniguez, L., Tweedle, M., Wilson, L. J., & Vickery, L. E. (1977) *Mechanisms of Oxidizing Enzymes* (Singer, T. P., & Ondarza, R. N., Eds.) Elsevier, Amsterdam, pp 221–238.

Powers, L., Chance, B., Leigh, J. S., Smith, J., Barlow, C., & Vik, S. (1979) *Developments in Biochemistry, 5: Cytochrome Oxidase* (King, T. E., Orii, Y., Chance, B., & Okunuki, K., Eds.) Elsevier, Amsterdam, pp 189–195.

Salmeen, I., Rimai, L., Gill, D., Yamamoto, T., Palmer, G., Hartzell, C. R., & Beinert, H. (1973) *Biochem. Biophys. Res. Commun. 52*, 1100–1107.

Salmeen, I., Rimai, L., & Babcock, G. T. (1978) *Biochemistry 17*, 800–806.

Schroedl, N. A., & Hartzell, C. R. (1977) *Biochemistry 16*, 4966–4971.

Seybert, D. W., Moffat, K., Gibson, Q. H., & Chang, C. K. (1977) *J. Biol. Chem. 252*, 4225–4231.

Shelnutt, J. A., Cheung, L. D., Chang, R. C. C., Yu, N.-T., & Felton, R. H. (1977) *J. Chem. Phys. 66*, 3387–3398.

Spaulding, L. D., Chang, C. C., Yu, N.-T., & Felton R. H. (1975) *J. Am. Chem. Soc. 97*, 2517–2525.

Spiro, T. G. (1974) *Acc. Chem. Res. 7*, 339–344.

Spiro, T. G., & Burke, J. M. (1976) *J. Am. Chem. Soc. 98*, 5482–5489.

Tweedle, M. F., Wilson, L. J., Garcia-Iniguez, L., Babcock, G. T., & Palmer, G. (1978) *J. Biol. Chem. 253*, 8065–8071.

Vanneste, W. H. (1966) *Biochemistry 5*, 838–848.

Verma, A. L., & Bernstein, H. J. (1974) *J. Raman Spectrosc. 2*, 163–173.

Warshel, A. (1977) *Annu. Rev. Biophys. Bioeng. 6*, 273–300.

Wikstrom, M. K. F., Harmon, H. J., Ingledew, W. J., & Chance, B. (1976) *FEBS Lett. 65*, 259–276.

Yamamoto, T., Palmer, G., Gill, D., Salmeen, I., & Rimai, L. (1973) *J. Biol. Chem. 248*, 5211–5213.

Yonetani, T. (1960) *J. Biol. Chem. 235*, 3138–3143.

Zobrist, M., & La Mar, G. N. (1978) *J. Am. Chem. Soc. 100*, 1944–1946.